Transition to Phase Synchronization of Chaos

Epaminondas Rosa, Jr.,* Edward Ott, and Mark H. Hess

Institute for Plasma Research, University of Maryland, College Park, Maryland 20742
(Received 20 October 1997)

Phase synchronization of chaos is studied using a modified Rössler system. By employing a lift of the phase variable (i.e., phase points separated by 2π are not considered as the same), the transition to phase synchronization is viewed as a boundary crisis mediated by an unstable-unstable pair bifurcation on a branched manifold, and the accompanying basin boundary structure is found to be of a new type. [S0031-9007(98)05362-9]

It is well known that two coupled chaotic oscillators can synchronize so that their evolutions become identical [1]. A distinct, but related chaos synchronization phenomenon can be developed in terms of a suitably defined [2] phase of a chaotic oscillator. For example, in the case of the Rössler oscillator [3], one can introduce an angle coordinate as a state space variable and regard it as the oscillator phase. Although this phase increases steadily with time, the rate of this increase will typically vary in a chaotic manner. This means that the rate of increase of the phase variable can be modeled as a mean steady drift with a (possibly small) superposed zero mean chaotic fluctuation. This chaotic fluctuation leads to diffusion of the phase superposed on the steady drift. It has been shown that this phase diffusion can be eliminated (*phase synchronization*) by the addition of a periodic pacing signal applied to the oscillator [2,4–7]. Furthermore, if the phase diffusion of the unpaced system is not too large, and if the imposed pacing frequency is close to matching the mean steady phase drift of the unpaced oscillator, then relatively small amplitudes of the pacing signal can completely eliminate phase diffusion. In the phase synchronized state, the oscillator remains chaotic, but its phase is in step with that of the pacing signal. That is, the phase difference between the pacing signal and the oscillator remains bounded by some appropriate constant fraction of 2π for *all time*. This is in contrast to the unsynchronized situation where the ensemble averaged diffusive phase spread continually increases as $(2D_\phi t)^{1/2}$, where D_ϕ is the phase diffusion coefficient, and t is time. Phase synchronization may, for example, be an important consideration in schemes for communication using the natural symbolic dynamics of chaos [8]. In particular, clock timing of information bits is typically a key factor in communication systems. Hence, the elimination of phase diffusion can be crucial in this application.

In this paper we study the transition of a paced chaotic oscillator from phase synchronized chaos to phase unsynchronized chaos as the pacing period varies. The mechanism of this transition has previously been treated in Ref. [6]. Our analysis uses a "lift" of the phase variable of the paced oscillator (the phase variable is considered on the real line rather than on the circle, and phase points separated by 2π are not considered as the same). In the lifted phase space the phase synchronization-desynchronization transition is an unstable-unstable pair bifurcation boundary crisis [9] on a two-dimensional branched manifold, and we find that the accompanying basin boundary structure is of a new type, different from the Weierstrass curve structure [10–12] previously seen in unstable-unstable pair bifurcation crises [9]. To our knowledge, this is the first documentation of an unstable-unstable pair bifurcation crisis occurring naturally in an ordinary differential equation system, rather than in maps designed for the study of such bifurcations [10–12].

The Rössler system [3] that we start with is $\dot{x} = -(y + z)$, $\dot{y} = x + 0.25y$, $\dot{z} = 0.90 + z(x - 6.0)$, here denoted by

$$d\mathbf{x}/dt = \mathbf{R}(\mathbf{x}). \tag{1}$$

The motion on the chaotic attractor of this system is such that orbits continually circulate around the z axis. Thus it is convenient to introduce cylindrical coordinates, $(x, y, z) \rightarrow (r, \phi, z)$, where $r = \sqrt{x^2 + y^2}$ and $\phi = \arcsin(y/r)$. Here we take the arcsin to be such that ϕ is continuous in time; i.e., it has no 2π jumps as t varies. With this convention ϕ increases continuously with t for orbits on the chaotic attractor. Note that, in our convention, the initial value of ϕ is ambiguous in that ϕ_0 and $\phi_0 \pm 2m\pi$ (m = integer) are physically equivalent. (However, we shall find it convenient to regard such physically equivalent initial conditions as distinct.) Another aspect of the chaotic attractor for this Rössler system is that, to a good approximation, it can be regarded as lying on a branched manifold. In particular, near $\phi/\pi \approx 2$ the attractor lies on a surface that has a ribbonlike structure; as ϕ decreases, the ribbon width stretches; as ϕ further decreases, the surface gradually folds widthwise, returning to its simple ribbon shape near $\phi \approx 0$.

We modify the system (1) by the multiplication of its right-hand side by a positive scalar function $S(\mathbf{x}, s)$ dependent on the parameter s, with $S(\mathbf{x}, 0) \equiv 1$. Thus,

the modified paced system becomes

$$d\mathbf{x}/dt = S(\mathbf{x}, s)\mathbf{R}(\mathbf{x}) + A\mathbf{P}(t). \qquad (2)$$

The term $A\mathbf{P}(t)$ is the periodic pacing signal, where $\mathbf{P}(t) = [0, \sin(2\pi t/T), 0]$. We take $S(\mathbf{x}, s) = 1 + s(r^2 - \bar{r}^2)$ and choose the parameter $\bar{r}$ to be the average value of r for $s = A = 0$.

For an unpaced system ($A = 0$) the presence of the function $S(\mathbf{x}, s)$ causes no change in the topological dynamics. In particular, the direction of the flow is still given by the direction of $\mathbf{R}$, so that the *paths* followed by orbits in the phase space are unaltered. Hence the branched manifold and any Poincaré surface of section map are not changed by $S(\mathbf{x}, s)$. The *speed* at which an orbit point moves along a path, however, is altered in a *position dependent* manner. Thus, $S(\mathbf{x}, s)$ can substantially change the phase diffusion D_ϕ of the unpaced chaotic system (even though the mean cycle time in ϕ is hardly changed). This is illustrated in Fig. 1 which shows the average $\langle(\phi - \langle\phi\rangle)^2\rangle$ over many orbits on the attractor of the unpaced system versus time for several s values. Notice how the slope (which is by definition $2D_\phi$) increases for increasing values of s. Thus, by varying the parameter s we are able to vary D_ϕ while keeping constant all topological aspects of the dynamics. We emphasize that, in our numerical experiments, use of the multiplier $S(\mathbf{x}, s)$ was essential: Because of the extremely small value of D_ϕ for Eq. (1) ($s = 0$ in Fig. 1), with the computer resources available to us, the phenomena we discuss here were not numerically observable in the unmodified Rössler equations (1) (although they very probably occur).

While, if $A = 0$, the topological dynamics is unchanged by $S(\mathbf{x}, s)$, this is not the case for $A \neq 0$. In particular, the required pacer amplitude to achieve synchronization is larger for larger D_ϕ. This is illustrated in Fig. 2 which shows regions of (A, T) parameter space corresponding to phase synchronized (open circles) and phase unsynchronized (filled circles) motions. Notice that the A scale in Fig. 2(b) for $s = 0.002$ is 10 times larger than the A scale in Fig. 2(a) for $s = 0$ [13]. For A and T values within the synchronization region, the pacing signal and the Rössler
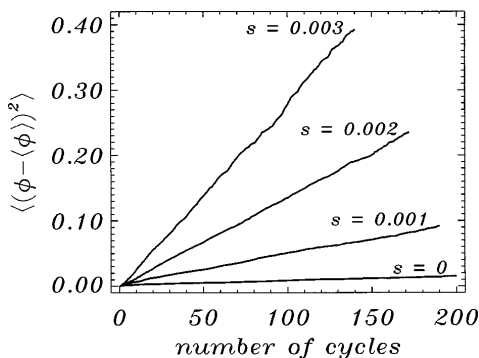
oscillator remain locked for all time. For values of A and T within the unsynchronized region, but near the synchronization boundary, pacer and oscillator experience long epochs of locking separated by intervals of short duration in which one of them quickly slips ahead a complete cycle. The duration of such locking varies erratically but has a well-defined average τ that diverges [6,9] as $T \to T_c$, where $T_c(A)$ is the critical value of the pacer period at the transition.

To proceed we consider $\theta = \phi - 2\pi t/T$, the phase difference between the oscillator and the pacer. Note that with our definition of ϕ, the quantity θ (like ϕ) is defined on the real line $-\infty < \theta < +\infty$ (rather than on the circle $0 \le \theta \le 2\pi$). With this definition phase synchronization corresponds to a chaotic attractor whose extent in θ is less than 2π. In fact, by the invariance of the system to the transformation $\theta \to \theta \pm 2\pi$, there is an infinite array of such attractors spaced by 2π in θ. For example, if the initial condition (r_0, z_0, θ_0) goes to one attractor, then $(r_0, z_0, \theta_0 + 2m\pi)$ goes to the attractor displaced from it by $2m\pi$. We now consider two such attractors denoted L and R, where L is located in $-\pi < \theta < \pi$ and R is located in $\pi < \theta < 3\pi$. To depict these attractors we use a stroboscopic surface of section (i.e., we examine r, z, θ at time $t = nT$ with n an integer). As we shall see, in this surface of section, the paced system attractor lies on a branched manifold similar to the
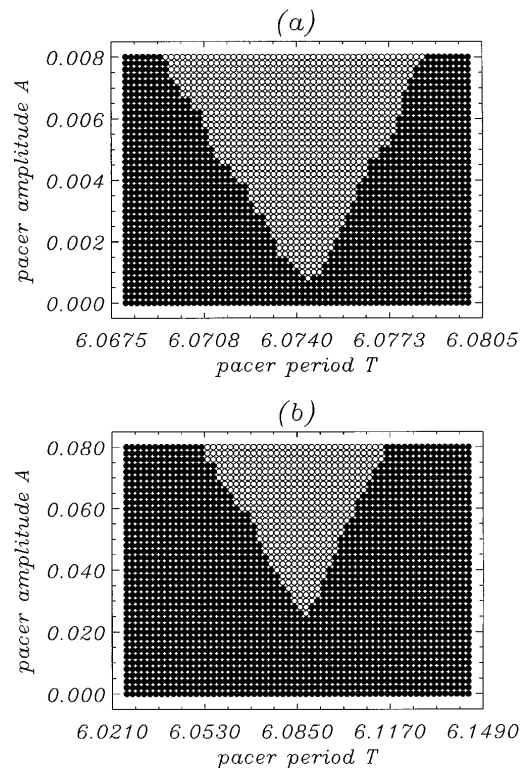
(a)

(b)

FIG. 2. A and T values for synchronized (open circles) and unsynchronized (filled circles) motion when (a) $s = 0$ and (b) $s = 0.002$.

FIG. 1. Time evolution of the variance.

branched manifold for the unpaced system. If A and T give synchronization, the strobed attractor does not fill the entire branched manifold but is localized in θ. Figure 3 for $T = 6.088$, $s = 0.002$, and $A = 0.130$ shows the attractors R and L in the stroboscopic surface of section, $t = nT$, along with points on the branched manifold that are in their respective basins of attraction. The values of the parameters T, s, and A for Fig. 3 correspond to the middle of the synchronization region in Fig. 2(b). Here we obtain our images of the basins of R and L *on the branched manifold* by sprinkling points in an appropriate volume of r, z, θ space and numerically seeing whether they go to attractor R or to attractor L. We then plot the resulting orbit locations a few cycles forward from the initial condition (typically four or five), thus allowing the orbits from the points initially sprinkled in the volume to approach the branched manifold. Taking the depicted R and L basins and attractors together, we can regard Fig. 3 as a *projection* of the two-dimensional branched manifold in (r, z, θ) onto (r, θ). Examining the branched manifold in the full three-dimensional space we find the following. Starting, say, at $\theta/\pi = 1.9$ and decreasing θ, the ribbon width stretches, becoming maximum at $\theta/\pi = 0.8$, and then folds widthwise as θ/π decreases from about 0.5 to 0.0, returning to its simple ribbon shape. We note that in the θ range of the basin boundary in Fig. 3, overlap due to projection of the branched manifold is absent.

To illustrate the mechanism of desynchronization consider Fig. 4 ($s = 0.002$, $A = 0.130$). As T decreases from a value in the middle of the synchronization tongue [$T = 6.088$, Fig. 4(a)] to values near the sychronization border [$T = 6.022 > 6.021 \approx T_c$ for Fig. 4(b)], we see that the R attractor and the L basin approach each other. At $T = T_c$, the attractor and the basin boundary touch. We observe [14] that this happens when a period three saddle orbit on the left edge of the R attractor coalesces with a period three repeller on the basin boundary. This process is called an unstable-unstable pair bifurcation crisis. (In an unstable-unstable pair bifurcation crisis an
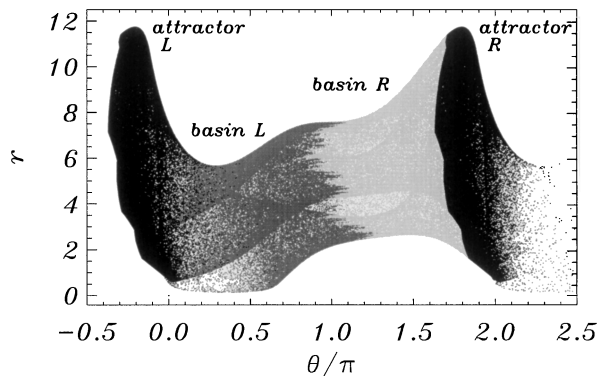
unstable periodic orbit on the attractor and an unstable periodic orbit of the same period on the attractor's basin boundary coalesce and annihilate [9].) Past the crisis, an orbit in the region of the former R attractor initially bounces around in that region for a long time, staying in synchronism with the pacer. After a while, however, it rather suddenly moves to the region of the former L attractor, undergoing a 2π phase slip between the oscillator and the pacer. It then stays in the region of the former L attractor, before experiencing another 2π phase slip in which it moves to the cell $-3\pi < \theta < -\pi$ containing another remnant attractor to the left of the L attractor, etc. In conformity with the theory of the unstable-unstable pair bifurcation crisis [9], and in agreement with the numerical results of the map model in Ref. [6], we numerically find that the mean time τ between 2π phase slips obeys the scaling $\log \tau \sim \text{const} \times |T - T_c(A)|^{-1/2}$. Figure 5 for T slightly less than $T_c(A)$ shows a plot of an orbit which was initialized in the region of the remnant R attractor. The sequence of 21 points shown (large dots, and we just labeled the first 12) correspond to the segment of the orbit around which it moves from the region of the remnant R attractor to the region of the remnant L attractor. Evidence for the mediating period three unstable-unstable pair bifurcation is clearly seen in the orbit motion between iterates 548 101 and 548 121 (large dots in Fig. 5) which closely follow period three motion, successively cycling through the three regions where the saddle-repeller coalescence has taken place [15].

The basin boundary structure we observe is illustrated in Fig. 6 [16] which shows a magnification of the boundary in Fig. 3. In the original studies of unstable-unstable pair bifurcation crises in Refs. [9], the basin boundary had the character of a fractal Weierstrass curve. In this case all points on the fractal boundary are *accessible* from both sides: for any point on the boundary, and any point in the interior of *either* basin, one can construct a connecting finite length curve that does not touch the boundary except at its end point. The structure we see in Fig. 6 is *not* of this type. Rather we see regions of the boundary that are rounded and appear to have many parallel striations. Further examination suggests that these striations
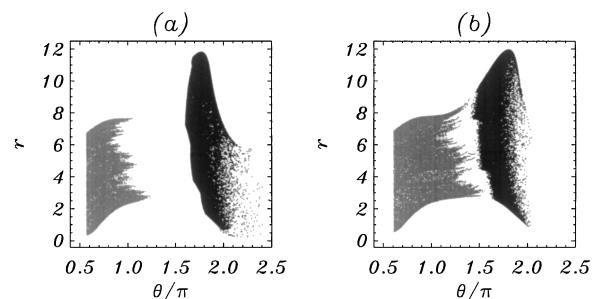

FIG. 3. L and R attractors ($T = 6.088$, $A = 0.130$, $s = 0.002$) and points on the branched manifold that are in their respective basins of attraction.

FIG. 4. R attractor and L basin for $s = 0.002$ and $A = 0.130$, with (a) $T = 6.088$ and (b) $T = 6.022$.
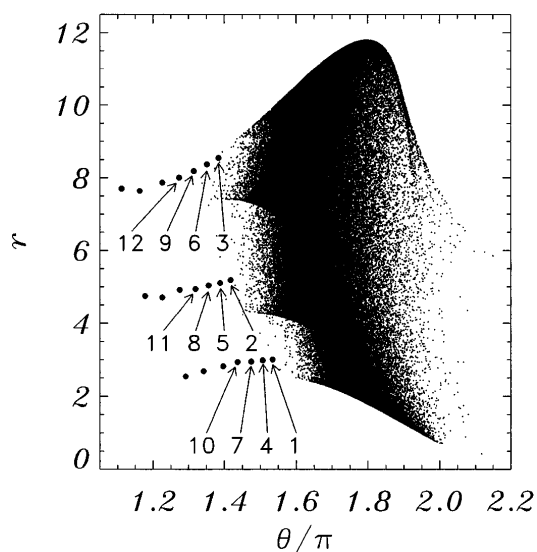
FIG. 5. Orbit initialized in the region of the remnant R attractor (T slightly less than T_c).

result from parts of the boundary that are essentially formed by a Cantor set of roughly parallel lines. Thus, there are points on the boundary (in fact, in an appropriate sense, most points) that are inaccessible from either basin, being "buried" under an infinite alternating sequence of ever narrower long basin strips accumulating on the boundary point from both sides. Such structures are commonly observed for fractal basin boundaries of two-dimensional invertible maps (e.g., the Hénon map) [11]. On the other hand, the fractal boundary in Fig. 6 is also fundamentally different from fractal basin boundaries observed for two-dimensional invertible maps [10,17]. In particular, for fractal basin boundaries of two-dimensional invertible maps there are typically no boundary points accessible from both sides. In contrast, in a future publication [14] we provide explicit examples of boundaries that are similar to the Fig. 6 boundary, and for these examples we can show that the boundary has an infinite fractal set of points (fractal dimension < 1) not in the rounded stri-
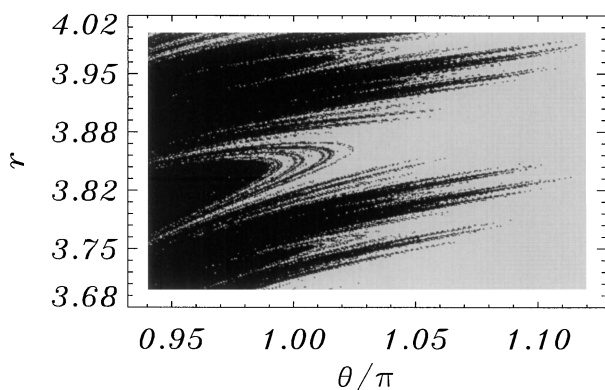

FIG. 6. Magnification of the basin boundary in Fig. 3.

ated regions that are accessible from *both* sides. Thus the boundary in Fig. 6 simultaneously incorporates features of both the aforementioned previously studied different basin boundary types.

---

*Permanent address: Departamento de Física, Universidade Federal do Paraná, Curitiba, PR, Brazil. Electronic address: erosa@glue.umd.edu

[1] L. M. Pecora and T. M. Carroll, Phys. Rev. Lett. **64**, 821 (1990); K. M. Cuomo, A. V. Oppenheim, and S. H. Strogatz, Int. J. Bifurcation Chaos **3**, 1629 (1993); R. Roy and K. S. Thornburg, Jr., Phys. Rev. Lett. **72**, 2009 (1994); D. J. Gauthier and J. C. Bienfeng, Phys. Rev. Lett. **77**, 1751 (1996); M. Ding and E. Ott, Phys. Rev. E **49**, 945 (1994); S. C. Venkataramani *et al.,* Phys. Rev. E **54**, 1346 (1996).
[2] M. G. Rosenblum, A. S. Pikovsky, and J. Kurths, Phys. Rev. Lett. **76**, 1804 (1996).
[3] O. E. Rössler, Phys. Lett. **57A**, 397 (1976).
[4] A. S. Pikovsky, Sov. J. Commun. Technol. Electron. **30**, 85 (1985).
[5] E. F. Stone, Phys. Lett. A **163**, 367 (1992).
[6] A. Pikovsky, G. Osipov, M. Rosenblum, M. Zaks, and J. Kurths, Phys. Rev. Lett. **79**, 47 (1997).
[7] U. Parlitz, L. Junge, W. Lauterborn, and L. Kocarev, Phys. Rev. E **54**, 2115 (1996).
[8] S. Hayes, C. Grebogi, E. Ott, and A. Mark, Phys. Rev. Lett. **73**, 1781 (1994); E. Rosa, Jr., S. Hayes, and C. Grebogi, Phys. Rev. Lett. **78**, 1247 (1997).
[9] C. Grebogi, E. Ott, and J. A. Yorke, Ergodic Theory Dynam. Syst. **5**, 341 (1985); Phys. Rev. Lett. **50**, 935 (1983).
[10] C. Grebogi, E. Ott, and J. A. Yorke, Physica (Amsterdam) **7D**, 181 (1983); Phys. Rev. Lett. **48**, 1507 (1982).
[11] S. W. McDonald, C. Grebogi, E. Ott, and J. A. Yorke, Physica (Amsterdam) **17D**, 125 (1985).
[12] E. Ott, *Chaos in Dynamical Systems* (Cambridge University Press, Cambridge, 1993), pp. 163–164.
[13] Also notice that the function $S(\mathbf{x}, s)$ has slowed the oscillator down, making its cycle time slightly longer.
[14] E. Rosa, Jr. and E. Ott (to be published).
[15] If we start in the middle of the tongue ($T \approx 6.088$) and *increase* T, similar phenomena occur, except that the crisis happens as a collision of the attractor with the basin boundary on its *right*. The (A, T) parameter values at the downward pointing tip of the locking region in Fig. 2 correspond to the case where the attractor just touches both its left and right basin boundaries simultaneously.
[16] Using the uncertainty dimension technique of Ref. [17] we numerically determine the fractal dimension of the basin boundary in Fig. 6 to be $d \approx 1.8$.
[17] C. Grebogi, S. W. McDonald, E. Ott, and J. A. Yorke, Phys. Lett. **99A**, 415 (1983).